Crystallization of GeO2 thin films into α-quartz

Zhou, Silang; Antoja-Lleonart, Jordi; Nukala, Pavan; Ocelík, Václav; Lutjes, Nick R.; Noheda, Beatriz

Published in:
Acta Materialia

DOI:
10.1016/j.actamat.2021.117069

Publication date:
2021

Different Environment Feedback in Fast-Slow Eco-Evolutionary Dynamics and Resulting Limit Cycles

Lulu Gong, *Student Member, IEEE*, and Ming Cao, *Senior Member, IEEE*

***Abstract*—The fast-slow dynamics of eco-evolutionary systems are studied, where we consider the feedback actions of environmental resources that are classified into those that are self-renewing and those externally supplied. We show that although these two types of resources are drastically different, the resulting closed-loop systems bear close resemblances, which include the same equilibria and their stability conditions on the boundary of the phase space, and the similar appearances of equilibria in the interior. After closer examination of specific choices of parameter values, we disclose that the global dynamical behaviors of the two types of closed-loop systems can be fundamentally different in terms of limit cycles: the system with the self-renewing resource undergoes a generalized Hopf bifurcation, and thus one stable and one unstable limit cycle can coexist; the system with the externally supplied resource only has the stable limit cycle.**

***Index Terms*—Game theory, stability of nonlinear systems.**

I. Introduction

TO STUDY complex biological and ecological systems, a range of mathematical models have been proposed, among which the Lotka–Volterra model [1], [2] and consumer-resource model [3], [4] have been playing prominent roles. The Lotka–Volterra model essentially describes the evolution of the predator and prey populations. The consumer-resource model covers a wider range of ecosystems, by taking into account diverse resource types. For another class of models, evolutionary game theory has served as the basis driven by the fitness consideration. Evolutionary game dynamics study the strategic evolution of one or multiple populations of individuals, where in the classic setting, the payoffs in each pairwise-interaction game are usually predetermined and specified by constant payoff matrices. Recently, an eco-evolutionary game model, introduced by evolutionary biologists in a series of seminal works [5], [6], [7], provides the description for the ecosystems from a dynamic-feedback game theoretical point of view. This model explicitly incorporates both games and resource dynamics into an integrated system, and the resulting coupled system dynamics are investigated accordingly.

The eco-evolutionary model is first proposed in [5], and is then generalized in [7] to consider different resource dynamics. In [7], it has been shown that the eco-evolutionary systems with renewable and decaying resources have similar behaviors in that their dynamics are qualitatively analogous. By varying the time-scale parameters, limit cycle behaviors are observed in both systems. Note that in the renewable resource case the population's actions are considered to consume the resource, while the population's actions will produce the resource in the decaying resource case.

In contrast, the resources are usually considered to be consumed by a population of consumers in the classic consumer-resource model. And the influence of different types of resources on the overall system properties is the usual subject of study [8]. Inspired by this, different from the existing eco-evolutionary models, in this work, we consider that all the strategic players in the population consume or harvest the resource with different harvest efforts. And two distinct and representative resource models, self-renewing and externally supplied resources, are studied. Self-renewing resources can represent biotic resources that grow logistically, while externally supplied resources are common among abiotic resources. The corresponding integrated eco-evolutionary models are suitable to study resource utilization and management in various ecological systems. It is worth noting that although our first model with the self-renewing resource is similar to the renewable resource model studied in [7], our second model is drastically different from the decaying resource model in [7] in that the strategists in our model are still considered to be consumers, which is consistent with the classic setting in consumer-resource models.

By extending the concept of resources dynamics, we study the eco-evolutionary dynamics under the different resource models using two-player two-strategy games. First, we show that these two systems bare some similarities in terms of boundary equilibria and their stability conditions. The two systems can have interior equilibria which can be continuous and thus infinite, and can also be two isolated points. Then, to

Manuscript received March 4, 2021; revised May 10, 2021; accepted June 1, 2021. Date of publication June 17, 2021; date of current version July 1, 2021. This work was supported in part by the European Research Council under Grant ERC-CoG-771687, and in part by the Netherlands Organization for Scientific Research under Grant NWO-vidi-14134. Recommended by Senior Editor F. Dabbene. *(Corresponding author: Lulu Gong.)*

The authors are with ENTEG, Faculty of Science and Engineering, University of Groningen, 9747 AG Groningen, The Netherlands (e-mail: l.gong@rug.nl; m.cao@rug.nl).

Digital Object Identifier 10.1109/LCSYS.2021.3089989

further analyze the stability of interior equilibria, we fix some parameters and conduct bifurcation analysis for one payoff parameter and the time-scale parameter. Through both one-parameter and two-parameter analyses, it is shown that both systems can exhibit Hopf bifurcations in the specific parameter conditions. However, the system with the self-renewing resource can further have the generalized Hopf bifurcation, which is impossible for the other system in the current setting. Therefore, in this situation it is natural for the first system to have a coexistence of two limit cycles, one stable and the other unstable, but the second system can only possess one stable limit cycle. We emphasize that although limit cycles have been identified in relevant eco-evolutionary research [7], [9], [10], [11], [12], unstable and double limit cycles have not been reported in the relevant studies so far. More importantly, we also implement analysis revealing how the two limit cycles can coexist through two-parameter bifurcation. It has been clarified that the time-scale difference and the payoff variation can have great influence on the eco-evolutionary dynamics, and as a result the two systems' behaviors become different and complicated.

The rest of this letter is organized as follows. Section II introduces the two eco-evolutionary systems. Section III shows some preliminary results in the general settings. Section IV further provides detailed bifurcation and stability analyses for the interior equilibria in some specific conditions, and numeric examples are given to illustrate the obtained theoretical results. Conclusions are drawn in Section V.

II. Problem Setup

A. Fast-Slow Eco-Evolutionary Systems

Consider in an infinite well-mixed population, the individuals play two-player matrix games with the strategy set $\mathscr{S} = \{1, 2, \ldots, n\}$. The payoffs for the players are affected by an external environmental factor. Using replicator equations to describe the evolution of strategies in the population and combining with the resource dynamics, we obtain the so-called *eco-evolutionary system* [7]

$$\begin{aligned} \in \dot{x}_i &= x_i[(A(m)x)_i - x^T A(m)x], i = 1, \ldots, n, \\ \dot{m} &= f(m) - h(x, m), \end{aligned} \tag{1}$$

where $x_i \in [0, 1]$ and $m \in \mathbb{R}_+$ respectively denote the frequency of strategy i and the amount of an environmental resource of interest; $x = [x_1, \ldots, x_n]^T$; $A(m)$ is the environment-dependent payoff matrix; $f(m)$ represents the intrinsic dynamics of the resource, and $h(x, m)$ captures the influence of the population's actions on the resource; ε accounts for the difference of time-scales between variables of the strategies and resource with $0 < \varepsilon \ll 1$ suggesting that the strategies evolve significantly faster than the resource.

B. Different Resource Dynamics

In reality, ecosystems can involve many types of resources, among which two typical and contrasting examples are biotic and abotic resources. The biotic resource, such as forests and animals, usually can self-replicate and thus grows logistically if the influence of the population is absent. Thus its intrinsic growth can be represented by a logistic function [3]

$$f_1(m) = m(1 - m/\kappa), \tag{2}$$

where κ is the carrying capacity of the resource. In contrast, the abiotic resource, such as minerals and small molecules, cannot self-replicate and is usually supplied externally to an ecosystem [8]. And its intrinsic dynamics can be captured by a liner function [8]

$$f_2(m) = K - wm, \tag{3}$$

where K is the constant flux from some external resource supplier, and w is the self-decay rate of the resource.

It is considered that all the strategists consume or harvest the resource, but different strategies have distinct harvest efforts $e_i > 0, e_i \neq e_j, \forall i, j \in \mathscr{S}$. And the function $h(x, m)$ has the form

$$h(x, m) = qm \sum_{i \in \mathscr{S}} e_i x_i,$$

where parameter q maps the harvest efforts into the rate of reduction in the resource.

When the intrinsic dynamics of the resource change, accordingly the feedback rules of the resource to the strategic dynamics are significantly different. In this work, we intend to investigate the eco-evolutionary dynamics under these two different resource feedback rules.

C. Normalized Models

We consider the typical two-strategy game, and assume the second strategy having higher harvest effort on the resource than the first, i.e., $e_2 > e_1 > 0$. We only need to focus on one strategy evolution because $x_1 + x_2 = 1$. For the self-renewing resource case, we can use the change of variable $r = \frac{m - \kappa(1 - qe_2)}{q\kappa(e_2 - e_1)}$ to normalize the resource variable such that r is confined in the unit interval $[0, 1]$. And we consider that the payoff matrix is linearly dependent on r and is a convex combination of payoff matrices of the two extreme cases when $r = 0$ and 1 respectively [12]. Then we have

$$A(r) = (1 - r)\begin{bmatrix} R_0 & S_0 \\ T_0 & P_0 \end{bmatrix} + r\begin{bmatrix} R_1 & S_1 \\ T_1 & P_1 \end{bmatrix}. \tag{4}$$

After a re-scaling of the system time by using $\tau = t/\varepsilon$, we obtain the eco-evolutionary system under self-renewing resource model as

$$\Sigma_s : \begin{cases} x' = x(1 - x)((b - a + d - c)xr + (a - b)x \\ \quad - (b + d)r + b), \\ r' = \varepsilon(1 - q(e_1 r + e_2(1 - r)))(x - r), \end{cases} \tag{5}$$

where $'$ represents the time derivative with respect to τ. For simplicity, we denote $a = R_0 - T_0$, $b = S_0 - P_0$, $c = T_1 - R_1$, and $d = P_1 - S_1$.

In a similar manner, for the externally supplied resource case, after the change of variable $r = \frac{(qe_1 + w)(m(qe_2 + w) - K)}{Kq(e_2 - e_1)}$ and the time re-scaling, we have the model

$$\Sigma_e : \begin{cases} x' = x(1 - x)((b - a + d - c)xr + (a - b)x \\ \quad - (b + d)r + b), \\ r' = \varepsilon(x(1 - r)(qe_1 + w) - r(1 - x)(qe_2 + w)). \end{cases} \tag{6}$$

Note that in both systems (5) and (6), it is assumed that $0 < e_1 < e_2 < 1/q$ due to its ecological implication [7].

III. Preparatory Analysis

For systems (5) and (6), the phase spaces are the unit square, i.e., $[0,1]^2$. There are 4 edges, of which the two edges, $\{(x,r)\in[0,1]^2 : x=0\}$ and $\{(x,r)\in[0,1]^2 : x=1\}$, are invariant under the two systems. The systems have the same equlibria on the edges, i.e., $(0,0)$ and $(1,1)$. These two equilibria correspond to the situations of full (resp. none) high consuming strategists and depleted (resp. abundant) resource. These two equlibria's stability is readily to check by the Jacobians. For system (5), the Jacobians at $(0,0)$ and $(1,1)$ are

$$\begin{bmatrix} b & 0 \\ \varepsilon(1-qe_2) & -\varepsilon(1-qe_2)\end{bmatrix}, \begin{bmatrix} c & 0 \\ \varepsilon(1-qe_1) & -\varepsilon(1-qe_1)\end{bmatrix}.$$

Thus, when $b<0$, $(0,0)$ is asymptotically stable, and it will be unstable if $b>0$. On the other hand, when $c<0$, $(1,1)$ is stable; if $c>0$ it will be unstable.

Similarly, for system (6), the Jacobians of the two edge equilibria are

$$\begin{bmatrix} b & 0 \\ \varepsilon(qe_1+w) & -\varepsilon(qe_2+w)\end{bmatrix}, \begin{bmatrix} c & 0 \\ \varepsilon(qe_2+w) & -\varepsilon(qe_1+w)\end{bmatrix},$$

which implies that the stability conditions for these two equilibria are the same as the conditions for system (5).

Systems (5) and (6) can also have some equilibria in the interior of the domain, i.e., $(0,1)^2$. For the interior equilibria, we have the following observation.

Lemma 1: Both systems (5) and (6) can have at most 2 isolated interior equilibria.

Proof: Consider system (5). Note that the term $(1-q(e_1r+e_2(1-r))$ is always positive for $r\in[0,1]$ because $0<e_1<e_2<1/q$. The interior equilibria can be solved by letting the right hand side of (5) be 0. Substituting $x=r$ yields

$$(b-a+d-c)r^2+(a-2b-d)r+b=0. \tag{7}$$

It can be checked that when $a=d, b=c=0$, system (5) has a continuum of equilibria: $\{(x,r)\in(0,1)^2 : x=r\}$. In other cases, (7) will have at most two real solutions. In view of the fact that the interior equilibrium has to be in $(0,1)^2$, system (5) can have at most 2 isolated interior equilibria.

For system (6), after calculations and the substitution of $x=\frac{(qe_2+w)r}{(qe_1+w)+q(e_2-e_1)r}$, one obtains

$$\begin{aligned}0=&[(b-a+d-c)(qe_2+w)-q(b+d)(e_2-e_1)]r^2\\&+[q(ae_2-2be_1-de_1)+w(a-2b-d)]r+b(qe_1+w).\end{aligned} \tag{8}$$

Similarly, one can conclude that when all the coefficients of (8) are 0, system (6) will have a set of equilibria $\{(x,r)\in(0,1)^2 : x=\frac{(qe_2+w)r}{(qe_1+w)+q(e_2-e_1)r}\}$; otherwise, system (6) has at most 2 isolated interior equilibria. ∎

In the following section, we carry out bifurcation analyses with respect to interior equilibria.

IV. Bifurcation and Stability Analyses

Due to the presence of too many parameters, it is difficult to analyze interior equilibria's stability collectively. Hence, in this section, we let some parameters be fixed specifically, and conduct bifurcation analysis for the interior equilibria with respect to two specific parameters. The payoff parameters a, b, d are chosen to be positive and c can vary along the real axis, so that we can focus on one payoff parameter. To distinguish the two strategies, their harvest efforts should be vastly different. The ecological parameters q and w are not important in our study. It has been identified that in such eco-evolutionary systems the time-scale difference is important, so it is also of interest to investigate its influence in our models. Therefore, we set $q=1$, $w=1$, $e_1=0.2$, $e_2=0.8$, and $a=0.2$, $b=0.1$, $d=0.4$. And $c\in\mathbb{R}$ and $\varepsilon\in(0,1]$ are the free parameters.

Now, we discuss the two systems separately.

A. Analysis of System Σ_s

1) Hopf Bifurcation: Denote the interior equilibria of system (5) by (x_s^*, r_s^*). As $x_s^*=r_s^*$ in this case, it is easy to determine the location of the interior equilibria by solving equation (7). As c varies, there can exist 0, 1 or 2 interior equilibria. When $c<-0.1$, there are no interior equilibria. When $c=-0.1$ and $c=0.3$, there is a unique interior equilibrium $(0.5,0.5)$. If $-0.1<c<0$, there exist two interior equilibria $(\frac{0.4\pm\sqrt{0.04+0.4c}}{2(0.3-c)}, \frac{0.4\pm\sqrt{0.04+0.4c}}{2(0.3-c)})$. And for $0\le c<0.3$ and $c\ge 0.3$, system (5) has a unique interior equilibrium $(\frac{0.4-\sqrt{0.04+0.4c}}{2(0.3-c)}, \frac{0.4-\sqrt{0.04+0.4c}}{2(0.3-c)})$.

Note that although $\frac{0.4-\sqrt{0.04+0.4c}}{2(0.3-c)}$ is not defined at $c=0.3$, from L'Hôpital's rule, one has $\lim_{c\to 0.3}\frac{0.4-\sqrt{0.04+0.4c}}{2(0.3-c)}=0.5$. Thus, we can summarize that there are two branches of interior equilibria: one branch, denoted by

$$(x_{s1}^*, r_{s1}^*) := \left(\frac{0.4+\sqrt{0.04+0.4c}}{2(0.3-c)}, \frac{0.4+\sqrt{0.04+0.4c}}{2(0.3-c)}\right), \tag{9}$$

only exists for $c\in(-0.1,0)$; the other branch exists for all $c\ge -0.1$, and is denoted by

$$(x_{s2}^*, r_{s2}^*) := \left(\frac{0.4-\sqrt{0.04+0.4c}}{2(0.3-c)}, \frac{0.4-\sqrt{0.04+0.4c}}{2(0.3-c)}\right). \tag{10}$$

Note that when $c<-0.1$, there exist no interior equilibria, and the equilibrium $(1,1)$ is locally stable because it has two negative eigenvalues. The edge equilibrium $(0,0)$ is a saddle point whose stable manifold is actually the edge $\{(x,r)\in[0,1]^2 : x=0\}$ because of the invariance. It can be checked that the vector fields in the close neighborhood of this edge all point inwards, which means a homoclinic orbit between the unstable and stable manifold of $(0,0)$ is impossible. Therefore, we have the following claim.

Lemma 2: $(1,1)$ is asymptotically stable in (5) for $c<-0.1$, and almost all trajectories starting from $[0,1]^2$ converge to it.

This result can be proved straightforwardly by applying the Poincaré-Bendixson theorem. The proof is omitted due to the space limit. This result implies that the full resource state can always be achieved provided that the payoff difference c is sufficiently small.

Now consider the Jacobian J_s^* at (x_s^*, r_s^*) which is given by

$$\begin{bmatrix}(x_s^*-x_s^{*2})((0.3-c)r_s^*+0.1) & (x_s^*-x_s^{*2})((0.3-c)x_s^*-0.5)\\ \varepsilon(0.6r_s^*+0.2) & -\varepsilon(0.6r_s^*+0.2)\end{bmatrix}. \tag{11}$$

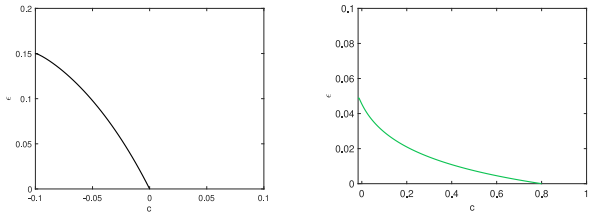

(a) T_0^s (b) T_0^e

Fig. 1. Zero trace curves.

The determinant and trace are given as below:

$$\det(J_s^*) = -\varepsilon(0.6x_s^* + 0.2)(x_s^* - {x_s^*}^2)(2(0.3-c)x_s^* - 0.4),$$
$$\mathrm{tr}(J_s^*) = (x_s^* - {x_s^*}^2)((0.3-c)x_s^* + 0.1) - \varepsilon(0.6x_s^* + 0.2).$$

It can be checked that the determinant of Jacobian at (x_{s1}^*, r_{s1}^*) is always negative, i.e.,

$$\det(J_{s1}^*) = -\varepsilon(0.6x_{s1}^* + 0.2)(x_{s1}^* - {x_{s1}^*}^2)\sqrt{0.4(0.1+c)} < 0$$

for $c \in (-0.1, 0)$. Then, it can be inferred the eigenvalues of J_{s1}^* are real and have different signs, which implies the instability of (x_{s1}^*, r_{s1}^*).

In contrast, the determinant of Jacobian at (x_{s2}^*, r_{s2}^*) is non-negative because $\det(J_{s2}^*) = \varepsilon(0.6x_{s2}^* + 0.2)(x_{s2}^* - {x_{s2}^*}^2)\sqrt{0.4(0.1+c)} \geq 0$ for $c \geq -0.1$. And only when $c = -0.1$, the determinant equals 0. When $\mathrm{tr}(J_{s2}^*) = 0$, the eigenvalues of J_{s2}^* will be purely imaginary if the corresponding determinant is not equal to 0. We let $\mathrm{tr}(J_{s2}^*) = 0$, and it results in

$$\varepsilon_c^s := \frac{(x_s^* - {x_s^*}^2)((0.3-c)x_s^* + 0.1)}{0.6x_s^* + 0.2} = \frac{55c + 30c\sqrt{10c+1} + \sqrt{10c+1} + 50c^2 - 1}{(10c-3)(3\sqrt{10c+1} - 10c + 9)}. \quad (12)$$

When c varies, (12) depicts a curve

$$T_0^s = \{(c, \varepsilon) : -0.1 < c < 0, \varepsilon = \varepsilon_c^s\} \quad (13)$$

in the parameter space (c, ε) as shown in Fig. 1 (a). On T_0^s, the trace of Jacobian of (x_{s2}^*, r_{s2}^*) is zero and the determinant is positive, thus it has purely imaginary eigenvalues, i.e.,

$$\lambda_{1,2}(J_{s2}^*)|_{\varepsilon_c^s} := \pm i\omega_0 = \pm i\frac{(30c + 10c\hat{c} + \hat{c} - 1)\sqrt{2\hat{c}(\hat{c}+3)}}{5(10c-3)^2}, \quad (14)$$

where $\hat{c} = \sqrt{10c+1}$. Then, for sufficiently small neighborhood of T_0^s, the Jacobian (11) has one pair of complex eigenvalues and can be denoted by

$$\lambda_{1,2}^s(J_{s2}^*) = \mu(c, \varepsilon) \pm i\omega(c, \varepsilon) \quad (15)$$

such that $\mu(c, \varepsilon) = 0$ and $\omega(c, \varepsilon) = \omega_0 > 0$ for c, ε on T_0^s.

Now, we take ε as the main parameter. The following theorem states that the interior equilibrium (x_{s2}^*, r_{s2}^*) undergoes a Hopf bifurcation.

Theorem 1: When $c \in (-0.1, 0)$, the interior equilibrium (x_{s2}^*, r_{s2}^*) of system (5) undergoes a *Hopf bifurcation* at ε_c^s defined by (12).

Proof: From Hopf bifurcation theorem [13, Th. 1], a Hopf bifurcation occurs at the parameter point where the equilibrium has a simple pair of pure imaginary eigenvalues and the derivative of the real parts of the eigenvalues is not zero. In (14), one has already obtained that the eigenvalues are purely imaginary when $c \in (-0.1, 0)$ and $\varepsilon = \varepsilon_c^s$.

Next, since the trace of the Jacobian is the sum of the eigenvalues, then in view of (11) and (15), one can check that the derivative of the real part of the eigenvalues is

$$\left.\frac{d\mu(c,\varepsilon)}{d\varepsilon}\right|_{\varepsilon_c^s} = \frac{10c - 9 - 3\sqrt{1+10c}}{10(3-10c)} < 0.$$

Thus, it is confirmed that the equilibrium (x_{s2}^*, r_{s2}^*) undergoes a Hopf bifurcation when the given condition is satisfied. ■

A Hopf bifurcation can be *supcritical* or *subcritical* depending on the sign of the *first Lyapunov coefficient* ℓ_1^s [13]. Actually, one can check that ℓ_1^s (the expression is given in the Appendix (21) which is obtained by using the algorithm in [14]) equals 0 when $c \approx -0.0889$. Moreover, as shown in Fig. 3 (a), ℓ_1^s is positive when $c \in (-0.1, -0.0889)$, and ℓ_1^s is negative when $c \in (-0.0889, 0)$. When $\ell_1^s > 0$, the Hopf bifurcation is subcritical such that an unstable limit cycle will be generated for ε in the vicinity of ε_c. In contrast, a stable limit cycle will bifurcate from (x_{s2}^*, r_{s2}^*) if $\ell_1^s < 0$ which implies the Hopf bifurcation is supercritical.

Next, we can clarify the stability of the interior equilibrium (x_{s2}^*, r_{s2}^*) as follows: when (c, ε) is above T_s^0, i.e., $c > -0.1$, $\varepsilon > \varepsilon_c^s$, the equilibrium is stable because of two negative eigenvalues; it is unstable when $-0.1 < c < 0$ and $\varepsilon < \varepsilon_c^s$ for the reason of two positive eigenvalues.

2) Generalized Hopf Bifurcation: Now we will study the case of $\ell_1^s = 0$, and we have to consider the *generalized Hopf bifurcation*. Note that $c \approx -0.0889$ when $\ell_1^s = 0$. In this case, we have $\varepsilon_c^s \approx 0.1429$, $\omega_0 \approx 0.0715$. Then, using the numerical tool Matcont, the *second Lyapunov coefficient* ℓ_2^s can be calculated $\ell_2^s = 4.8221 \times 10^{-5} \neq 0$. To confirm the generalized Hopf bifurcation at parameter values $(-0.0889, 0.1429)$, the regularity condition has to be satisfied [14]. One can verify this condition by checking if the determinant of Jacobian matrix of the map $(c, \varepsilon) \to (\mu(c, \varepsilon), \ell_1^s(c, \varepsilon))$ near $(-0.0889, 0.1429)$ is nonzero, namely

$$\det\begin{pmatrix} \frac{\partial \mu}{\partial c} & \frac{\partial \mu}{\partial \varepsilon} \\ \frac{\partial \ell_1^s}{\partial c} & \frac{\partial \ell_1^s}{\partial \varepsilon} \end{pmatrix}\Bigg|_{(-0.0889, 0.1429)} \neq 0.$$

The computation of ℓ_2^s and $\det(\cdot)$ is tedious and complicated, so the process is omitted here. Instead, we use the numeric bifurcation plot to show that the generalized Hopf bifurcation does take place, as shown in Fig. 2 (f). Intuitively, the generalized Hopf bifurcation implies that the system has two limit cycles of opposite stability properties for some (c, ε) near the bifurcation point $(-0.0889, 0.1429)$.

For a given payoff parameter c, one can see that the timescale difference has an important influence on the system behaviors. There is a critical value of ε, such that the interior equilibrium's stability changes as ε crosses it. It results in the existence of stable or unstable limit cycles in the phase space of system (5) for the neighborhood of the bifurcation point. The stable limit cycle corresponds to the dynamic coexistence of the strategies and resource characterized by the sustained oscillation. In comparison, the unstable limit cycle separates the phase space, which implies that the system's

trajectories starting from different regions can behave drastically differently. Moreover, for a certain c, unstable and stable limit cycles could coexist, which makes the dynamic behaviors even more complicated. This behavior corresponds to an interesting dynamic bistable phenomenon for an equilibrium and a limit cycle, which can also be observed in other population dynamics models [15].

Next, we study system (6) and the procedure is quite similar.

B. Analysis of System Σ_e

Denote the interior equilibria of (6) by (x_e^*, r_e^*). Solving (8) yields the r-coordinate of (x_e^*, r_e^*). When $c < -1/60$, there are no solutions to (8), and thus the interior equilibrium does not exist. When $-1/60 \le c < 2/15$ and $c > 2/15$, one has $r_e^* = \frac{0.6-\sqrt{0.04+2.4c}}{2(0.4-3c)}$. As $c = 2/15$, (8) has a single solution $r_e^* = 1/3$. Similarly, we can denote the r-coordinate of the equilibrium uniformly by $r_e^* = \frac{0.6-\sqrt{0.04+2.4c}}{2(0.4-3c)}$, because of $\lim_{c\to 2/15} \frac{0.6-\sqrt{0.04+2.4c}}{2(0.4-3c)} = 1/3$.

Because $x_e^* = 1.8r_e^*/(1.2 + 0.6r_e^*)$ in this case, there is a unique interior equilibrium

$$(x_e^*, r_e^*) := \left(\frac{3\sqrt{60c+1}-9}{\sqrt{60c+1}+60c-11}, \frac{0.6-\sqrt{0.04+2.4c}}{2(0.4-3c)} \right), \tag{16}$$

when $c \ge -1/60$. Otherwise, there are no interior equilibria, in which case obviously one has the analogous claim as in Lemma 2. It means that the full resource state is also approachable under a similar condition of the payoff difference as in system (5), which also confirms the similarity between the two systems.

Next, we evaluate the Jacobian J_e^* of (x_e^*, r_e^*), i.e.,

$$\begin{bmatrix} (x_e^* - x_e^{*2})((0.3-c)r_e^* + 0.1) & (x_e^* - x_e^{*2})((0.3-c)x_e^* - 0.5) \\ \varepsilon(1.2 + 0.6r_e^*) & -\varepsilon(1.8 - 0.8x_e^*) \end{bmatrix}. \tag{17}$$

Following the same procedure, we obtain the determinant and trace of J_e^*

$$\det(J_e^*) = 3\varepsilon(x_e^* - x_e^{*2}) \frac{120cr_e^* - 15r_e^* + 20cr_e^{*2} - r_e^{*2} + 14}{50(r_e^* + 2)},$$
$$\mathrm{tr}(J_e^*) = (x_e^* - x_e^{*2})((0.3-c)r_e^* + 0.1) - \varepsilon(1.8 - 0.8x_e^*).$$

The sign of $\det(J_e^*)$ is determined solely by the numerator $120cr_e^* - 15r_e^* + 20cr_e^{*2} - r_e^{*2} + 14$. Substituting $r_e^* = \frac{0.6-\sqrt{0.04+2.4c}}{2(0.4-3c)}$ into it yields $\frac{33c'-525cc'-215c+1800c^2c'+1500c^2+17}{2(15c-2)^2}$, where $c' = \sqrt{60c+1}$. It can be checked that it is always positive for $c \ge -1/60$, which implies that $\det(J_e^*)$ is positive. Similarly we can obtain the zero trace curve

$$T_0^e = \{(c, \varepsilon) : -1/60 < c < 4/5, \varepsilon = \varepsilon_c^e\},$$
$$\varepsilon_c^e := \frac{(x_e^* - x_e^{*2})((0.3-c)r_e^* + 0.1)}{1.8 - 0.8x_e^*}$$
$$= \frac{37cc' - 125c + 4c' - 165c^2c' + 255c^2 + 900c^3 + 1}{(2-15c)(12cc' - 330c - c' + 1080c^2 + 23)}. \tag{18}$$

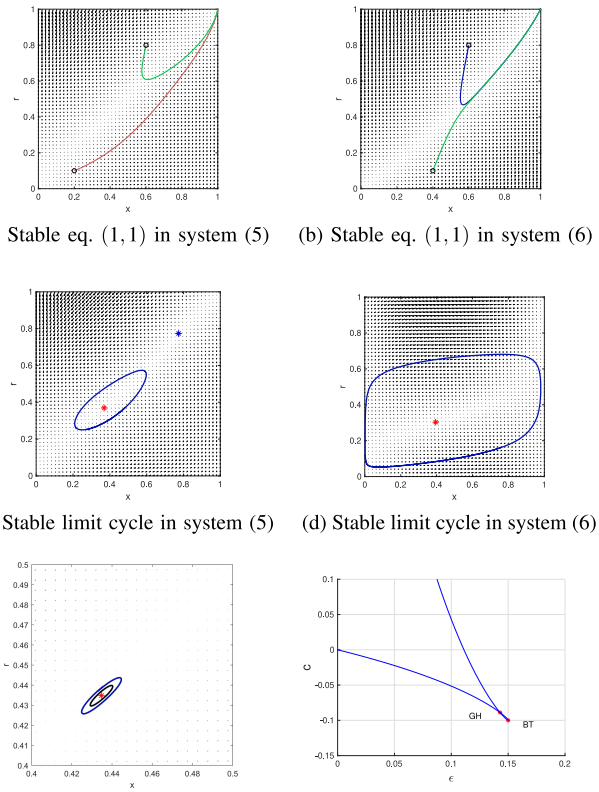

(a) Stable eq. $(1,1)$ in system (5) (b) Stable eq. $(1,1)$ in system (6)

(c) Stable limit cycle in system (5) (d) Stable limit cycle in system (6)

(e) Coexistence of two limit cycles in system (5) (f) Two-parameter bifurcation plot

Fig. 2. The parameters are as follows: (a). $\varepsilon = 0.2$, $c = -0.15$; (b). $\varepsilon = 0.2$, $c = -0.05$; (c). $\varepsilon = 0.125$, $c = -0.05$; (d). $\varepsilon = 0.02$, $c = 0.2$; (e). $\varepsilon = 0.145$, $c = -0.091$. (f). GH is the generalized Hopf bifurcation, BT is the Bogdanov-Takens bifurcation (not covered in this work).

T_0^e is shown in the parameter space (c, ε) as Fig. 1 (b). Clearly, on T_0^e, (x_{s2}^*, r_{s2}^*) has purely imaginary eigenvalues:

$$\lambda_{1,2}(J_e^*)|_{\varepsilon_c^e} := \pm i\nu_0,$$
$$\nu_0 = \Big(\big(72(300c + 5c' - 55)(60c - 10cc' + 3c' - 13) \cdot (99c' - 1575cc' - 645c + 5400c^2c' + 4500c^2 + 51) \cdot (15cc' - 75c + c' + 1)^2\big) / (25(15c-2) \cdot (300c - 40)(3c' - 540c + 63)(60c + c' - 11) \cdot (60cc' - 630c - 11c' + 1800c^2 + 61)^2) \Big)^{1/2}. \tag{19}$$

Then, for sufficiently small neighborhood of T_0^e, the Jacobian (17) has one pair of complex eigenvalues denoted by

$$\lambda_{1,2}^e(J_e^*) = \delta(c, \varepsilon) \pm i\nu(c, \varepsilon) \tag{20}$$

such that $\delta(c, \varepsilon) = 0$ and $\nu(c, \varepsilon) = \nu_0 > 0$ for c, ε on T_0^e. Now, we have the following result.

Theorem 2: When $c \in (-1/60, 4/5)$, the interior equilibrium (x_e^*, r_e^*) of system (6) undergoes a *supercritical Hopf bifurcation* at ε_c^e as defined in (18).

Proof: The proof of is similar to that of Theorem 1. From (19), one knows that the eigenvalues are a pair of pure imaginary eigenvalues, i.e., $\pm i\nu_0$, when $c \in (-1/60, 4/5)$ and $\varepsilon = \varepsilon_c^e$. In view of (17) and (20), one obtains the derivative of the real part of the eigenvalues $\frac{d\delta(c,\varepsilon)}{d\varepsilon}|_{\varepsilon_c^e} = \frac{3(c'-180c+21)}{10(60c+c'-11)} < 0$.

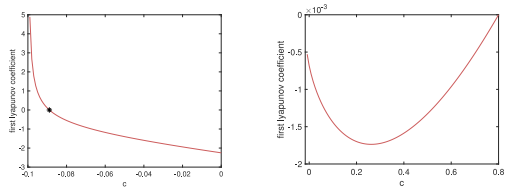

(a) ℓ_1^s (b) ℓ_1^e

Fig. 3. The plots of the first Lyapunov coefficient. (a). the asterisk is the point where $\ell_1^s = 0$. (b). $\ell_1^e < 0$.

Thus, the equilibrium (x_{s2}^*, r_{s2}^*) undergoes a Hopf bifurcation at ε_c^e for $c \in (-1/60, 4/5)$. Next, the negative first Lyapunov coefficient at (x_{s2}^*, r_{s2}^*) (as shown in (22) and Fig. 3 (b)) confirms the supercritical Hopf bifurcation. ■

The same argument can be used to clarify the stability of the interior equilibrium (x_e^*, r_e^*), i.e., when $c > -1/60$, and $\varepsilon > \varepsilon_c^e$, the equilibrium is stable; it is unstable when $-1/60 < c < 4/5$ and $\varepsilon < \varepsilon_c^e$.

In system (6), similar Hopf bifurcation and stable limit cycles as in system (5) can take place, which again confirms the time-scale difference's important impact. However, the existence of double limit cycles is not possible due to the negative first Lyapunov coefficient, no matter what value c takes. The nonexstence of unstable and double limit cycles reveals the significant difference of eco-evolutionary dynamics caused by these two different environmental resource feedback.

Fig. 2 gives some simulations to show the behaviors of systems (5) and (6), where a two-parameter bifurcation plot for system (5) is also presented.

V. Conclusion

In this letter, we have studied the eco-evolutionary dynamics under two different resource models. Our main results have shown that the dynamic behaviors of the corresponding systems have similarities, but can be qualitatively different in the specialized conditions. They are able to exhibit limit cycles when the time-scale difference between the strategy and resource variables is sufficiently large. In particular, the system under the self-renewing resource feedback can display two limit cycles of opposite stability when the payoff parameters vary. Our work highlights the complexity of the environmental and strategic dynamics induced by the time-scale difference and payoff variation. The obtained results may provide valuable insight for relevant studies.

There are a number of interesting future directions such as studying multiple populations [16], [17] and resources, e.g., different resources exist at the same time. Moreover, we have focused on a specific case, so robustness of the discovered dynamic behaviors is needed to be studied. From numerical simulations in [18], one may conclude that the results reported in this letter hold even in the larger parameter space.

Appendix

$$\begin{aligned}\ell_1^s = {} & -5000000(c-0.3)^2(((30c-1)\hat{c} - 100(c+0.1)^2)^{1/2}(c+0.1)\cdot \\ & (-50c^2 + 30\hat{c}c - 55c + \hat{c} + 1)^{1/2}((-3/20c^3 + 9/8c^2 - 681/500c - 567/1250)\hat{c} \\ & + c^4 - 13c^3/4 + 221c^2/200 + 1737c/500 + 117/250) + ((4500c^3 \\ & + 2300c^2 - 35c + 2)\hat{c} - 5000c^4 - 15500c^3 - 1950c^2 - 25c + 2)^{1/2}\cdot \\ & ((-37500c^4 + 154000c^3 - 108125c^2 - 65130c - 5184)\hat{c} + 100000c^5 \\ & - 247500c^4 - 118500c^3 + 376225c^2 + 90390c + 5184)/100000))/ \\ & ((10c + 3\hat{c} - 9)^2(10c - 3\hat{c} + 1)^2(50^2 - 30\hat{c}c + 55c - \hat{c} - 1)\cdot \\ & (100c^2 - 30\hat{c}c + 20c + \hat{c} + 1)). \end{aligned} \tag{21}$$

$$\begin{aligned}\ell_1^e = {} & 151165440000000000000000000(c-2/15)^4(c-1/4)^6\cdot \\ & c(c-4/5)^5c'(3((3/10c^3 + 19/200c^2 - 1/1500c + 1/45000)c' \\ & + c^4 + 119c^3/60 + 203c^2/1800 - 1/45000)c(60c + 7c' + 1)^{1/2}/20 \\ & + \sqrt{2}((11/40c^5 - 73/7200c^4 - 989/216000c^3 + 29/120000c^2 \\ & + 1/200000c - 1/3000000)c' + (c + 1/60)(c^5 + 77/60c^4 \\ & - 1043/3600c^3 + 43/2000c^2 - 9/10000c + 1/50000)))/ \\ & ((60c + 7c' + 1)^{3/2}(-11 - c' + 60c)^2(10cc' - 3c' + 60c - 13)^4\cdot \\ & (100c'c^2 + 6000c^3 - 185cc' - 5000c^2 + 24c' + 715c - 24)^4v_0^3). \end{aligned} \tag{22}$$

References

[1] A. J. Lotka, *Elements of Physical Biology*. Baltimore, MD, USA: Williams Wilkins, 1956.

[2] V. Volterra, "Variazioni e fluttuazioni del numero d'individui in specie animali conviventi," in *Memoria della Reale Accademia Nazionale dei Lincei, Anno CCCCXXIII, II* (Fluctuations in the Abundance of a Species Considered Mathematically), vol. 118, Nature, 1926, pp. 558–560.

[3] R. MacArthur and R. Levins, "The limiting similarity, convergence, and divergence of coexisting species," *Amer. Naturalist*, vol. 101, no. 921, pp. 377–385, 1967.

[4] P. Chesson, "Macarthur's consumer-resource model," *Theor. Population Biol.*, vol. 37, no. 1, pp. 26–38, 1990.

[5] J. S. Weitz, C. Eksin, K. Paarporn, S. P. Brown, and W. C. Ratcliff, "An oscillating tragedy of the commons in replicator dynamics with game-environment feedback," *Proc. Nat. Acad. Sci.*, vol. 113, no. 47, pp. E7518–E7525, 2016.

[6] Y.-H. Lin and J. S. Weitz, "Spatial interactions and oscillatory tragedies of the commons," *Phys. Rev. Lett.*, vol. 122, Apr. 2019, Art. no. 148102.

[7] A. R. Tilman, J. B. Plotkin, and E. Akçay, "Evolutionary games with environmental feedbacks," *Nat. Commun.*, vol. 11, p. 915, Feb. 2020.

[8] W. Cui, R. Marsland, and P. Mehta, "Effect of resource dynamics on species packing in diverse ecosystems," *Phys. Rev. Lett.*, vol. 125, Jul. 2020, Art. no. 048101.

[9] D. G. Rand, D. Tomlin, A. Bear, E. A. Ludvig, and J. D. Cohen, "Cyclical population dynamics of automatic versus controlled processing: An evolutionary pendulum," *Psychol. Rev.*, vol. 124, no. 5, p. 626, 2017.

[10] J. D. Bever, K. M. Westover, and J. Antonovics, "Incorporating the soil community into plant population dynamics: The utility of the feedback approach," *J. Ecol.*, vol. 85, no. 5, pp. 561–573, 1997.

[11] J. Henrich, "Demography and cultural evolution: How adaptive cultural processes can produce maladaptive losses: The tasmanian case," *Amer. Antiquity*, vol. 69, no. 2, pp. 197–214, 2004.

[12] L. Gong, W. Yao, J. Gao, and M. Cao, "Limit cycles in replicator-mutator dynamics with game-environment feedback," *IFAC-PapersOnLine*, vol. 53, no. 2, pp. 2850–2855, 2020.

[13] J. Guckenheimer and P. Holmes, *Nonlinear Oscillations, Dynamical Systems and Bifurcations of Vector Fields*. New York, NY, USA: Springer,2000.

[14] Y. A. Kuznetsov, *Elements of Applied Bifurcation Theory*. New York, NY, USA: Springer, 2004.

[15] P. Yu and W. Lin, "Complex dynamics in biological systems arising from multiple limit cycle bifurcation," *J. Biol. Dyn.*, vol. 10, no. 1, pp. 263–285, 2016.

[16] L. Gong, J. Gao, and M. Cao, "Evolutionary game dynamics for two interacting populations in a co-evolving environment," in *Proc. 57th IEEE Conf. Decis. Control*, 2018, pp. 3535–3540.

[17] Y. Kawano, L. Gong, B. D. O. Anderson, and M. Cao, "Evolutionary dynamics of two communities under environmental feedback," *IEEE Control Syst. Lett.*, vol. 3, no. 2, pp. 254–259, Apr. 2019.

[18] L. Gong and M. Cao, "Different environment feedback in fast-slow eco-evolutionary dynamics," 2021. [Online]. Available: arXiv:2105.04659.